

# Photoelectrochemical Degradation of Methyl Orange Using TiO<sub>2</sub>/Ti Films Prepared via Sol-Gel Technique

Zulkarnain Zainal,\* Chong Yong Lee, Anuar Kassim,  
Mohd Zobir Hussein, Nor Azah Yusof

Department of Chemistry, University Putra Malaysia, 43400 UPM Serdang, Malaysia.  
Tel.: +603 89466810, Fax: +603 89435380, E-mail: zulkar@science.upm.edu.my.

Received: 10-04-2006

## Abstract

TiO<sub>2</sub> thin films have been prepared using the sol-gel method. The chemically modified sol-gel precursor solution was obtained by the addition of polyethylene glycol and diethanolamine to the titanium alkoxide precursor. Hydrolysis and polycondensation reactions of the precursors in the presence of water were controlled. Electrochemical assisted photocatalytic degradation system has been investigated on a model pollutant, methyl orange dye. Properties of the films were determined as a function of calcination temperatures by surface morphology, X-ray diffraction and photoelectrochemical studies. The photoelectrochemical degradation rate is almost linearly increased with an increased in applied bias potential. The improved in percentage of degradation for about 30% for every increases of 0.5 V was observed for potential range between 0 V and 1.0 V. However, direct electrochemical oxidation of dye begins to occur at potential of 1.5 V and above due to dark current as indicated from current-potential curve behaviour. Introduction of more concentrated dye leads to a decrease in the photodegradation percentage but the rate of photoelectrochemical degradation was almost the same. Larger photocatalyst coated area gives higher degradation rate but showed less charge density.

**Keywords:** Photoelectrochemical degradation, calcination, methyl orange

## 1. Introduction

Titanium dioxide is a well-known semiconductor photocatalyst that has been explored by researchers worldwide. It acts as a multifunctional material with several applications.<sup>1,2</sup> Among all, the most famous applications of TiO<sub>2</sub> is in wastewater and air treatments.<sup>3–7</sup> TiO<sub>2</sub> can acts very well as photocatalyst which can degrade or mineralise toxic and hazardous compounds in aqueous solution to the unharmed compounds such as H<sub>2</sub>O, CO<sub>2</sub> and other inorganic substances.<sup>8,9</sup> It is also used as self-cleaning coating for facades and other surfaces exposed to the polluted air.<sup>6,7</sup>

In the context of wastewater treatment, TiO<sub>2</sub> has been investigated as a photocatalytic material in two major systems namely suspension and immobilized. However, difficulty of its recovery and separating the photocatalysts from the degraded reaction mixture which needs centrifugation or filtration processes makes the immobilized system more preferable in practical point of view. The need for post-treatment is eliminated in the immobilised system which is an economically advantage.<sup>10</sup> TiO<sub>2</sub> have been successfully immobilized on various supporting ma-

terials such as glass, ceramic, quartz, titanium plates, silica, glass fibers, zeolites and alumina.<sup>6,10–11</sup>

Illumination of photocatalyst with light energy  $\geq 3.2$  eV (TiO<sub>2</sub> bandgap energy) can promote the electron from valence band to the conduction band, thereby creating electron-hole pairs. Hydroxide ions in the solution react with the holes to produce the hydroxyl radicals which are strong oxidising agents. However, at the same time electron-hole recombination rapidly occur and decrease photodegradation efficiency.<sup>12,13</sup>

Efforts have been made to enhance the photodegradation efficiency by minimizing the charge recombinations. This aim could be achieved by applying an external bias potential to the catalyst placed on the electrode.<sup>14</sup> The applied external bias potential reduce charge recombination and generated electron on TiO<sub>2</sub> films can flow to the counter electrode in the cell assembly during irradiation. Consequently, only the electrically conducting supporting materials can be used as substrate (electrodes).<sup>15–17</sup>

Several methods to immobilize photocatalyst on substrate such as sol-gel process, chemical vapour deposi-

tion, electrophoretic coating and sputtering have been reported.<sup>6,10</sup> In this study, sol-gel method was chosen due to several advantages such as possibility of varying film properties, low process cost and easier preparation compared to other oxide film techniques. Surface morphology, crystallinity and electrochemical characteristic of the films prepared via dip-coating the titanium substrate into modified titanium alkoxide sol-gel solution were investigated. Photocatalytic degradation was carried out on methyl orange dye as a model pollutant together with applying bias voltage to verify the photocatalytic efficiency of the TiO<sub>2</sub> films.

## 2. Experimental

### 2.1. Preparation of Precursor Solutions

The precursor solution for TiO<sub>2</sub> sol was prepared using the system that containing titanium tetraisopropyl-orthotitanate, polyethylene glycol (molecular weight,  $M_w = 2000$ ), diethanolamine, ethanol and water as reported by Kato.<sup>18–20</sup> Modifications were made on molar ratio between precursors and adding sequences. The molarity of alkoxide in the ethanol was 0.94 mol L<sup>-1</sup>. The molar ratio of diethanolamine to the alkoxide was one. The concentration of polyethylene glycol and water to alkoxide was 6 wt. % and 0.8 wt %, respectively. The polyethylene glycol was mixed with the ethanol before adding other chemicals in the following sequences; diethanolamine, titanium tetraisopropyl orthotitanate and water. The mixture was stirred in a sealed vessel for several hours at room temperature. The resulting sol gel was colourless and transparent.

### 2.2 Preparation of TiO<sub>2</sub> Thin Films

Titanium plates (5 × 2 cm<sup>2</sup>) were used as a conducting supporting material for TiO<sub>2</sub> layers. The plate was polished by silicon carbide paper (Bioanalytical system PK-4 polishing kit) and cleaned with acetone in an ultrasonic bath for 15 min. The treated Ti plate was dried in an oven at 100 °C for 15 min and then manually dip-coated with sol-gel solution and left to dry at room temperature. The speed of both dipping the titanium plate into and pull out from sol-gel solution is about 2 s cm<sup>-2</sup>. The coated electrode was heated at 100 °C for 5 min in oven followed by subsequent dip-coating. An area with size of 1.5 × 2.0 cm<sup>2</sup> at the top was left uncoated to provide the area of the electrical contact. This step was repeated several times until the amount of TiO<sub>2</sub> catalyst loaded was approximately 2.00 × 10<sup>-3</sup> g (required 5 layers, total thickness estimated by using SEM is about 0.4 μm). Finally, the plate was annealed at desired calcinations temperature in a Thermolyne 21100 furnace for 2 h.

### 2.3 Analytical Measurements

The photoelectrochemical measurements were carried out in the two-compartment cell equipped with a quartz plane window. The anode and cathode electrodes were separated by Polytetrafluoroethylene (PTFE) 0.45 μm membrane. The working electrode was a TiO<sub>2</sub>/Ti plate and the counter electrode was a platinum plate (1 cm<sup>2</sup>). All the potentials were specified to the Ag/AgCl reference electrode which was connected to the assembly via a salt bridge. The electrode potentials and photocurrents were recorded using AMEL general-purpose potentiostat-galvanostat Model 2049. Meanwhile, a potentiostat EG&G Princeton Applied Research (PAR) VersaStat driven by model 270 Electrochemical Analysis System software with PC control was used for linear sweep voltammetry (LSV) and cyclic voltammetry (CV) measurements. The temperature of the reactor solutions was maintained at 313 K throughout the experiments by using a water jacket circulation system. Tungsten halogen projector lamp (Osram, 300 W and 120 V) was used as light source. The halogen lamp has a spectra emission ranging from 360 nm to 830 nm. The light source was placed 8 cm away from the sample. Photoreactor cell was filled with 120 ml methyl orange solution (10 ppm) with 0.1 mol L<sup>-1</sup> NaCl as supporting electrolyte. The samples were withdrawn every 30 min thereafter for a period of 120 min. The concentration of the methyl orange in the solution was determined by measuring the absorbance values using UV/Vis Perkin Elmer Lambda 20 Spectrophotometer. Scanning electron microscopy was performed on SEM JSM 6400 JEOL Scanning Microscope to analyse the morphology and surface characteristics of the coated TiO<sub>2</sub> films. X-ray diffractometry (XRD) analysis was employed to identify the crystalline phases on the films. This technique was performed using Shimadzu XRD 6000 Diffractometer for 2θ ranges from 2° to 60° with Ni-Filter and Cu-Kα radiation ( $\lambda = 1.54056 \text{ \AA}$ ).

## 3. Results and Discussion

### 3.1. Characterization of TiO<sub>2</sub> Films

The scanning electron micrographs of TiO<sub>2</sub> particulate films heat-treated at temperatures of 100 °C and 500 °C are shown in Figure 1. Cracks appeared on the surface of the film after being heat-treated at temperature 100 °C which resulting from the endothermic evaporation process involving organic precursors and externally or internally bound water molecules. Large differential evaporation, stresses and variation of pore sizes in the gel are also reported to be factors causing the layer to crack.<sup>21</sup> In addition, the appearance of cracks resulted in poor films' adhesion, where the films were found to peeled off easily when pass through a steady stream of water. Thus, higher heat-treatment temperature is required to get better adhesion property.

## Scanning Electron Microscopy Studies

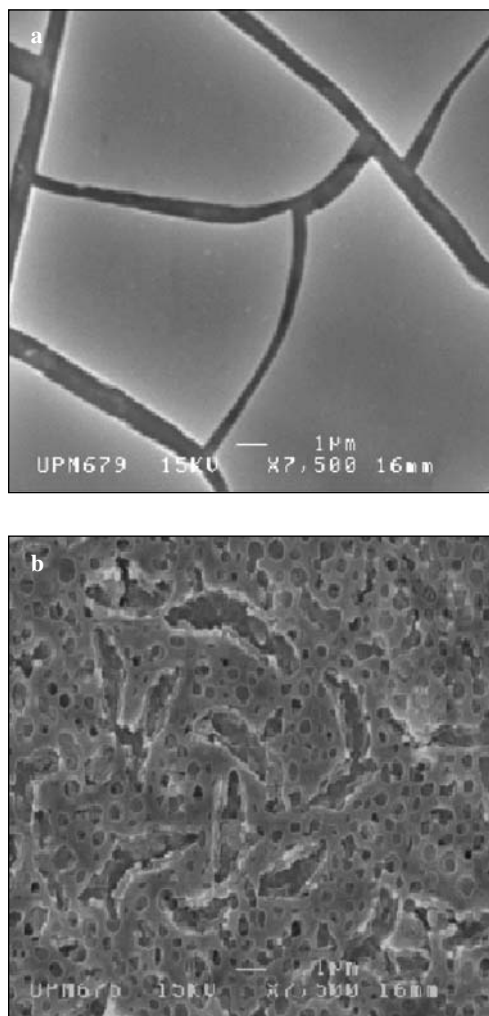


**Figure 1.** Surface morphologies images of thin films prepared at heat-treatment temperatures of (a) 100 °C and (b) 500 °C (magnification = 7500×).

The surface morphology changed when the films were heat-treated at higher temperature. This could be attributed to the transformation of TiO<sub>2</sub> phase. Samples heat-treated at 500 °C appeared rather porous with the diameter of pore less than 1.0 μm. It is believed that release of organic parts either through evaporation or decomposition of organic matters in the sol-gel significantly contributes to this appearance.<sup>22</sup> Tiny fractures and cracks could be seen which occurred due to less differential evaporation, nevertheless the same contraction and stress still suffered by the sol-gel during aging and drying process.

The XRD patterns of the films heat-treated at 100 °C to 500 °C are shown in Figure 2. Apart from the substrate (Ti) peaks, no other peaks were obtained at 300 °C and below. The peaks belonging to anatase and rutile TiO<sub>2</sub> phases exist when the samples were heated at 400 °C and above. The most pronounced peak is observed at  $d = 3.51 \text{ \AA}$

## X-ray Diffraction Measurements

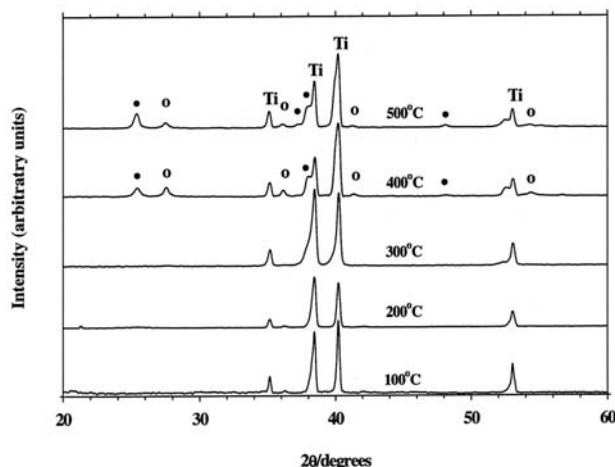


**Figure 2.** XRD patterns of samples heat-treated at different temperatures (\* = anatase, o = rutile, Ti = titanium substrate).

which corresponds to (101) plane of anatase TiO<sub>2</sub>. Better crystallinity was obtained for sample heated at 500 °C. A rutile peak appeared at  $d = 3.24 \text{ \AA}$ , which correspond to (110) plane for samples heated at 400 °C and 500 °C. Several broad and low intensity anatase and rutile peaks were also observed.

The crystallite size of TiO<sub>2</sub> thin films can be deduced from XRD line broadening using the Scherrer equation:<sup>23</sup>

$$L = \frac{K\lambda}{\beta \cos \theta}$$

where  $L$  is the crystallite size of TiO<sub>2</sub> thin films,  $K$  is a constant (0.94),  $\lambda$  is the wavelength of X-ray ( $\text{CuK}\alpha = 1.54056 \text{ \AA}$ ),  $\beta$  is the true half-peak width, and  $\theta$  is the half diffraction angle of the centroid of the peak in degree. Any contributions to broadening due to the non-uniform stress were neglected and the instrumental line width in the XRD apparatus was subtracted.<sup>24</sup> The average crystallite sizes of anatase and rutile TiO<sub>2</sub> phases are found to be 16 and 17 nm, respectively.

## 3.1.3 Electrochemical Characteristics

The electrochemical behaviour of the films was characterised in 10 ppm methyl orange solution. Sodium chloride solution of 0.1 mol L<sup>-1</sup> was added as a supporting electrolyte. Figure 3 shows the photocurrent obtained for TiO<sub>2</sub> electrode heat treated at different temperatures between 100 °C and 500 °C. The voltammograms show that photocurrent values increase with increasing annealing temperature. Electrodes heated at 300 °C and below show lower photocurrent value compared to 400 °C and 500 °C. This is due to better crystallinity of TiO<sub>2</sub> when heated at higher temperature as shown by the XRD results. Beside

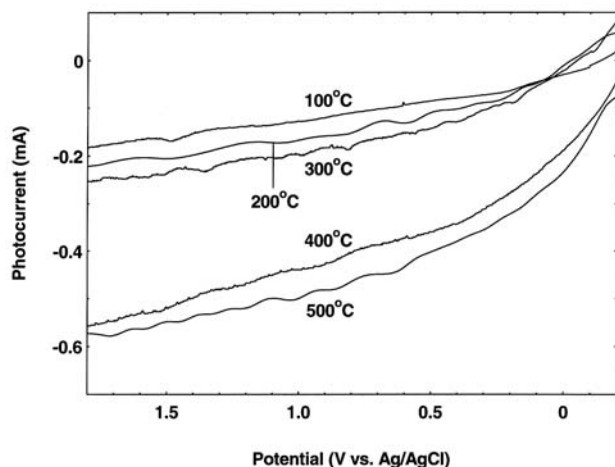


**Figure 3.** Linear sweep voltammograms for electrodes prepared at different calcination temperatures in 10 ppm methyl orange solution containing  $0.1 \text{ mol L}^{-1}$  NaCl and under illumination with 300 W halogen lamp. The scan rate was  $20 \text{ mV s}^{-1}$ .

that, large quantity of organic component covering the surface of sample heat-treated at lower temperature may cause the reduction of light penetrated and reached the electrode reaction zones, consequently reducing the photocurrent values. The behaviour might also be due to considerable amount of defects or surface states existing on the electrodes that increases the film resistance.<sup>25</sup>

Bulk resistance is the natural ohmic resistance of a p-type or n-type semiconductor. If the bulk resistance is too high, the quantum efficiency will become lower due to the decrease of electrical gradient across the depletion and thin space charge layer.<sup>26–27</sup> This consequently decreases the generation of photocurrent. Thus, the reduction of  $\text{Ti}^{4+}$  to  $\text{Ti}^{3+}$  in the film by the decomposed organic matter or unburned free carbons during heating process contributes

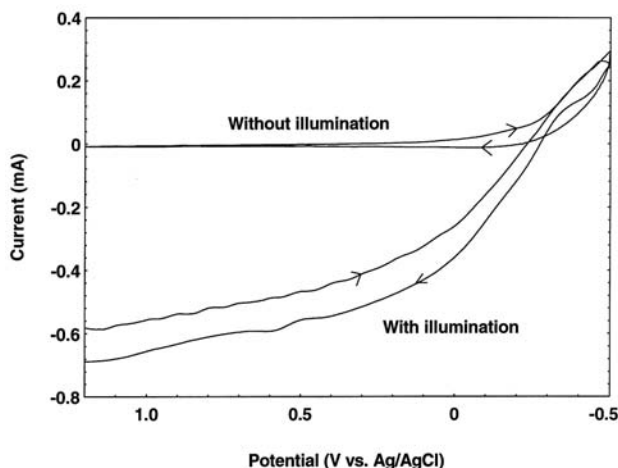
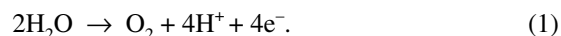


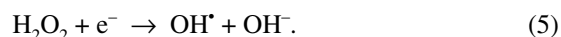
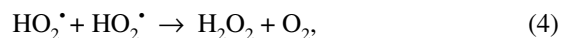
**Figure 4.** Cyclic voltammograms for electrode prepared at  $500^\circ\text{C}$  in 10 ppm methyl orange solutions containing  $0.1 \text{ mol L}^{-1}$  NaCl in dark and under illumination of a 300 W halogen lamp. The scan rate was  $20 \text{ mV s}^{-1}$ .

to the decrease of the film resistance. The presence of  $\text{Ti}^{3+}$  ions would dominate both the photoelectrochemical reaction at the surface and bulk electrical conductivity by the formation of donor level in the conduction band of  $\text{TiO}_2$ .<sup>26,28</sup> Besides that, strong adhesion between the film and the substrate was achieved when higher temperature was applied and successfully reduced the bulk resistance.

Figure 4 shows the cyclic voltammograms for the electrode under illumination and in dark. It was observed that in the presence of light, anodic photocurrent for the oxidation process starts at  $-0.25 \text{ V}$ . This photocurrent may be attributed to oxygen evolution reaction which could produce the superoxides ( $\text{O}_2^{\cdot-}$ ).<sup>29</sup> Oxygen is produced via water oxidation on  $\text{TiO}_2$  electrode as shown below:<sup>2</sup>



The superoxides formed through photochemical process could help in generation of additional amount of hydroxyl radicals as shown in equation below:



Non-irradiated system shows no anodic current response. This observation shows that dye oxidation did not occur at potential range of  $-0.25 \text{ V}$  to  $1.2 \text{ V}$  in the dark. Therefore, high photoelectrocatalytic activity of  $\text{TiO}_2$  coupled with the oxygen evolution reaction might be very favourable for the photoelectrochemical degradation process.

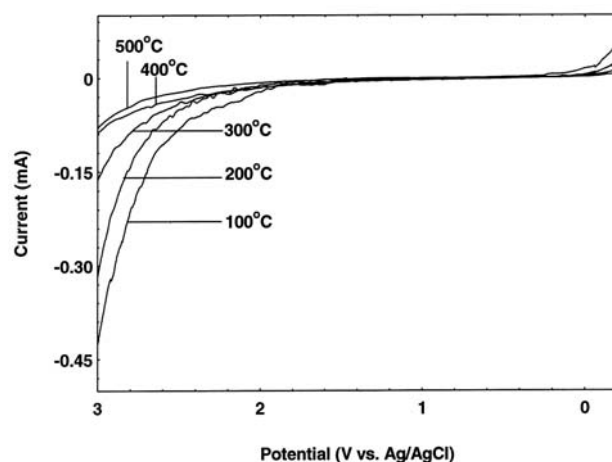


**Figure 5.** Linear Sweep Voltammograms for electrodes prepared at different calcinations temperatures in 10 ppm methyl orange solutions containing  $0.1 \text{ mol L}^{-1}$  NaCl in dark. The scan rate was  $20 \text{ mV s}^{-1}$ .

Figure 5 shows the I–V characteristic of the electrode heat-treated with different temperatures. No illumination was applied in order to identify the potential value for direct electrochemical oxidation. It can be observed that dark current begin to occur at potential 1.5 V onwards. This potential is the starting point of electrochemical oxidation process. However, heat-treatment process on electrodes at 400 °C and 500 °C successfully reduced the value of dark current. This might be due to improvement of TiO<sub>2</sub> adhesion on titanium plate at higher calcination temperatures. This agrees with the report by Sun et al.,<sup>30</sup> who stated the excellent adhesion of the film could suppress the dark current at high potential. Thus, the dark current recorded at potential higher than 1.5 V is due to direct oxidation of dye and water. Therefore, the photocurrent response of potential higher than 1.5 V is a result of direct oxidation of dye and photooxidation of dye and water.

### 3.2. Photodegradation Study

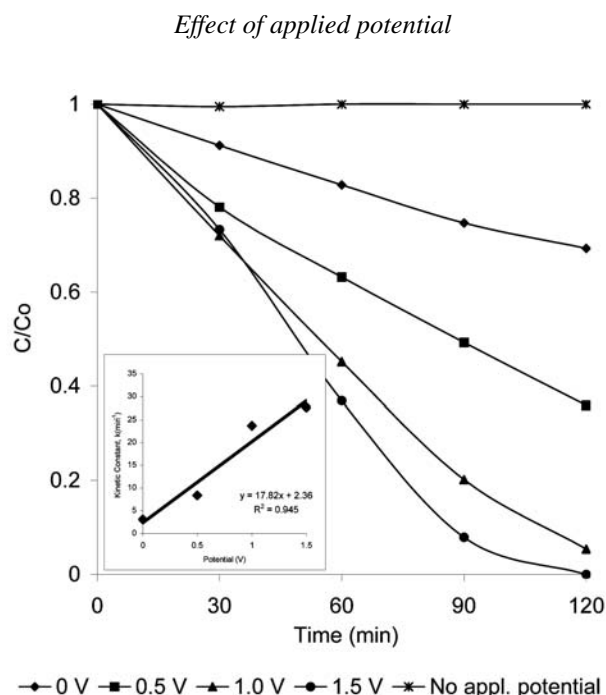


**Figure 6.** Methyl orange degradation dependence on applied potential during illumination of the samples. Inset shows the pseudo first order kinetic constant vs. the voltage of electrical bias potential.

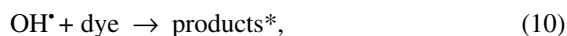
The effect of external bias potential on the methyl orange photoelectrochemical degradation process is shown in Figure 6. The experimental results of photoelectrochemical degradation are reported as ratio of ( $C/C_0$ ) versus illumination time ( $t$ ), where  $C_0$  is the initial concentration of dye and  $C$  is the concentration at time,  $t$  (min). An increase in the applied potential enhanced the photoelectrochemical degradation rate. Applying

the bias potential from 0.0 V to 1.5 V (vs. Ag/AgCl) increased the percentage of degradation of dye in 120 min from 31% to 100. The control experiment was run without applying external potential which shows absolutely no photodegradation. Besides that, another control experiment was carried out by applying similar potentials in the dark. The experimental result in line with voltammetry study (I–V result, refer to Figure 5) where generated current is zero at potential range of 0.0 V to 1.5 V, means direct electrochemical oxidation did not occurred at those potentials. Extended study by applying potential higher than 1.5 V shows the occurrence of electrochemical oxidation of dye.

The bias potential significantly promotes the photoelectrochemical degradation rates from 0.0 V to 1.0 V, but starts to decrease at potential between 1.0 V and 1.5 V. This trend can be explained from the I–V characteristic curve for electrode heat-treated at 500 °C as shown in Figure 3. Photocurrent increased gradually from potential 0.0 V to 1.0 V but recorded small increased from 1.0 V to 1.5 V. This result shows that the reaction rates were enhanced by applying bias potential, but reach saturation when bias potential is higher than 1.0 V.

The increase in photocurrent at high anodic potential resulted from more frequent excitation of electrons from valence to conduction band, when illuminated by light. This is due to the reduction in the recombination rate of electron-hole pairs generated at TiO<sub>2</sub>/dye solution interface. The increase in dye degradation rate was due to the production of more holes for the reaction on electrode surface (TiO<sub>2</sub>/Ti(h)<sub>surf</sub>) or generation of more strong oxidizing agents. The chloride ions, which had been introduced as supporting electrolyte will also be adsorbed onto TiO<sub>2</sub> surface to produce dissolved oxidants such as Cl<sup>•</sup> and Cl<sub>2</sub><sup>•-</sup>.<sup>31</sup> The competition between the adsorption of OH<sup>-</sup> ions and Cl<sup>-</sup> on the semiconductor surface is pH dependent.<sup>32</sup> Dye pollutants will be degraded or mineralised into unharmed products such as H<sub>2</sub>O, CO<sub>2</sub> and other mineral acids. The reactions occurring on working and counter electrode are proposed by Eqs.6–13:

At illuminated working electrode (WE):



At dark counter electrode (CE):



products\*:  $\text{CO}_2$ ,  $\text{H}_2\text{O}$ , mineral acids and unarmful inorganic compounds.

The application of bias potential can promote better charge separation in  $\text{TiO}_2$  particles which can improve the efficiency of photodegradation process. When an anodic bias is applied, a potential gradient developed within the film drive away the photogenerated holes and electrons in opposite directions.<sup>12,13,16</sup> The increase in photoelectrochemical degradation rate may be attributed to positive potential bias which lowers the Fermi energy level of the supporting substrate, thus allowing more electron transfer from the film to the supporting substrate. This results in generation of higher photocurrent.

Electrochemical assisted photodegradation process also increases mass transfer of negatively charged species toward the positive  $\text{TiO}_2$  working electrode via electromigration through electrostatic effect. This helps reduce mass transfer limitation imposed by the reduction of catalyst surface area to volume ratio encountered when using an immobilized catalyst.<sup>33</sup>

As shown in inset in Figure 6, there is an almost linear relationship between bias potential and the first order kinetic constant  $k$  where the first order kinetic constant  $k$  increased with an increase in applied bias potential. The

relation between the applied voltage,  $V$  and kinetic-order constant can be summarized using the below equation:

$$k = 17.82 V + 2.36. \quad (14)$$

From Eq.6, the  $k$  value increases by applying higher bias potential. Therefore, photoelectrochemical degradation increases linearly along with potential applied if the reaction pathway remains the same throughout the experiment. However this experiment condition is quite difficult to achieve since an increase of dark current is observed at potential 1.5 V onwards which indicates the beginning of direct electrochemical oxidation of dye in the solution. Therefore, this equation is applicable only for bias potential 1.5 V or less. Another study is needed to determine the effect of potential towards both photoelectrochemical and electrochemical oxidation of dye at potential higher than 1.5 V.

The effect of methyl orange concentration towards the photoelectrochemical degradation is shown in Figure 7. As the initial dye concentrations was increased, more dye molecules competes to be absorbed onto the surface of the electrode. However due to the limitation of amount of catalyst loaded, light intensity, illumination time and temperature, only certain amount of dye could be degraded. This resulted in low percentage of photodegradation at higher dye concentration. The similar trend of the effect of initial concentration towards the photodegradation rates was observed elsewhere.<sup>34</sup> The amount of OH and Cl radicals, which are the primary oxidant formed on the surface of  $\text{TiO}_2$  is limited by the above factor, so the relative number of free radicals attacking the dye molecules decreases with increasing amount of dye molecules.

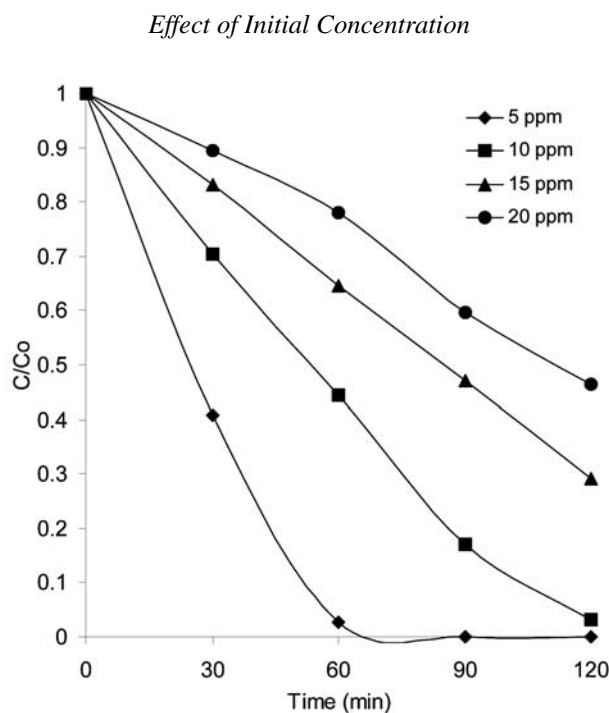


**Figure 7.** Methyl orange degradation dependence on dye initial concentrations. Potential was fixed at a 1.0 V and electrodes were illuminated using a 300 W halogen lamp.

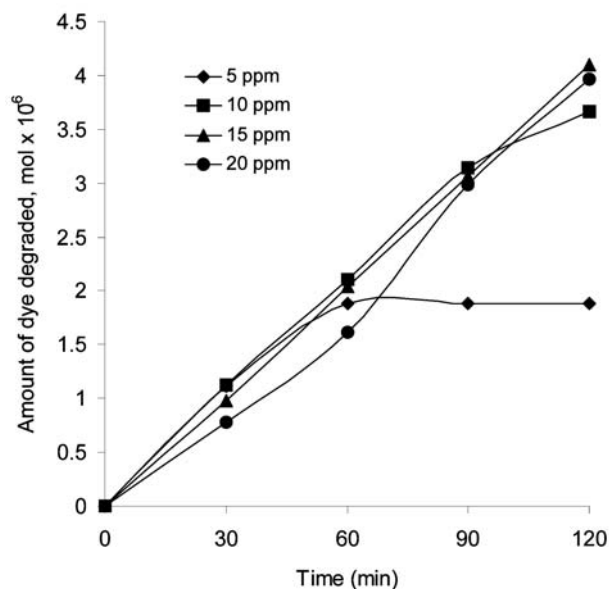


**Figure 8.** Amount of methyl orange degraded variation with different initial dye concentration.

Besides that,  $\text{TiO}_2$  requires sufficient photon energy to generate electron-hole pairs as the major sources of producing the oxidising agents or sites. Since the dye solution became more intense with increasing dye concentrations, the quantity of light with suitable photon energies that entering the solution and reached the electrode will become less. This behaviour could be seen in Figure 8 where dye with initial concentration of 20 ppm show slower degradation. On the contrary, the decrease of dye concentration will enhance the photon energy from the light source reaching the reaction zone on the electrode. This will increase the formation of active site and free radicals due to high charge carrier generation, thereby the amount of dye degraded increase.

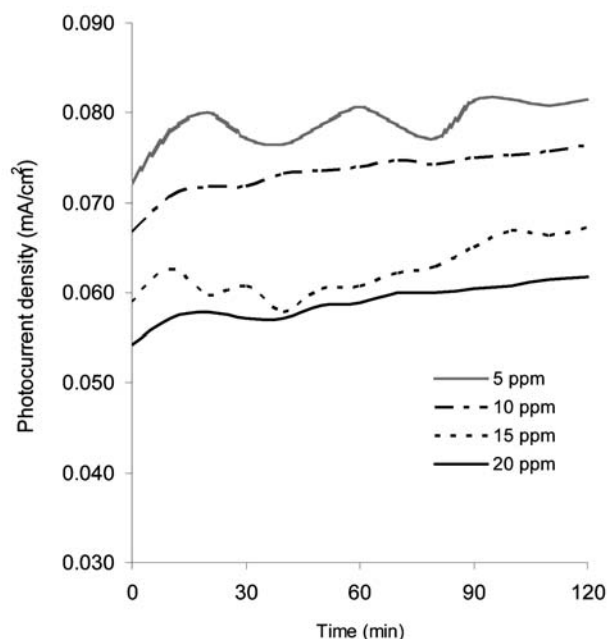


**Figure 9.** Photocurrent density recorded for the electrode immersed in methyl orange with different initial dye concentrations. Potential was fixed at a 1.0 V and illumination source was a 300 W halogen lamp.

**Table 1: Table 1.** Calculation of percentage and half time of methyl orange degradation based on Figure 7. Accumulated charges,  $Q$ , were calculated corresponding to the photocurrent recorded vs. time.

Initial concentration (ppm)	Degradation (%)	Half time (min)	Accumulated charges, $Q$ (C)
5	100	25	66.26
10	96.81	54	61.73
15	70.85	86	52.37
20	53.62	112	49.51

Photocurrent density recorded at different concentration is shown in Figure 9. The value of photocurrent density is low at high solution concentrations. This obser-

vation verified that the light path reaching the electrode decreases when higher concentration of dye is used. In this case, the photocurrent density indicates the reduction of photocatalytic reaction on electrode. The results show that the decrease in the photocurrent value decreases the amount of charges accumulated in the same period of irradiation time. Consequently, photodegradation percentage was also decreased.

The effect of coated electrode area on the effectiveness of the photoelectrochemical degradation and photocurrent generated was examined by coating  $\text{TiO}_2$  on elec-

#### Effect of coated electrode area

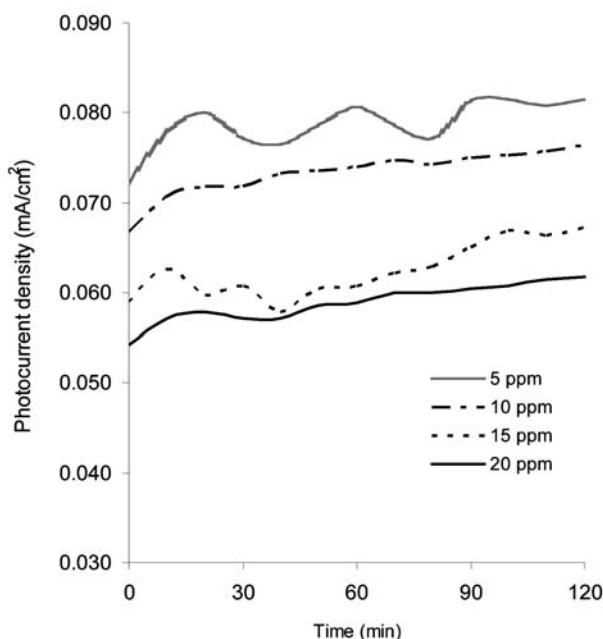


**Figure 10.** The methyl orange dye degradation dependence on the photocatalyst coated area of electrode. Potential was fixed at a 1.0 V and electrodes were illuminated with a 300 W halogen lamp.

trode with different coated area. The results showed that increasing  $\text{TiO}_2$  coated area could improve the methyl orange degradation rate as shown in Figure 10. This observation shows that the photoelectrochemical processes leading to degradation reaction occur on the surface of the electrode.

The larger electrode coated area confirms the fact that more  $\text{TiO}_2$  is involved in catalysing the reaction. The experimental result agrees with the literature finding,<sup>35</sup> which concluded that the increase in  $\text{TiO}_2$  catalyst loading would increase the number of active sites and thereby increase the rate of removal.

The charge density for different coated electrode area was investigated in this study. The charge density is defined as the amount of charges per coated area and is shown in Figure 11.

$$\text{Charge density} = \frac{\text{Accumulated charges, } Q \text{ (C)}}{\text{Area of catalyst coated, } A \text{ (cm}^2\text{)}} \quad (15)$$

The charge density increases with decreasing catalyst coated area. This indicates that charge produced per area is higher for smaller electrodes. It is possible to infer that the electrode with smaller electrode coated area is more efficient in generating the photocurrent. However, this information is not enough to justify the effectiveness of the electrodes for photodegradation. The relationship between the charge density and photodegradation could be better understood by evaluating the amount of dye successfully degraded per coated area. This is defined as specific removal:

$$\text{Specific removal} = \frac{\text{Amount of dye degraded (mol)}}{\text{Area of catalyst coated, } A \text{ (cm}^2\text{)}} \quad (16)$$

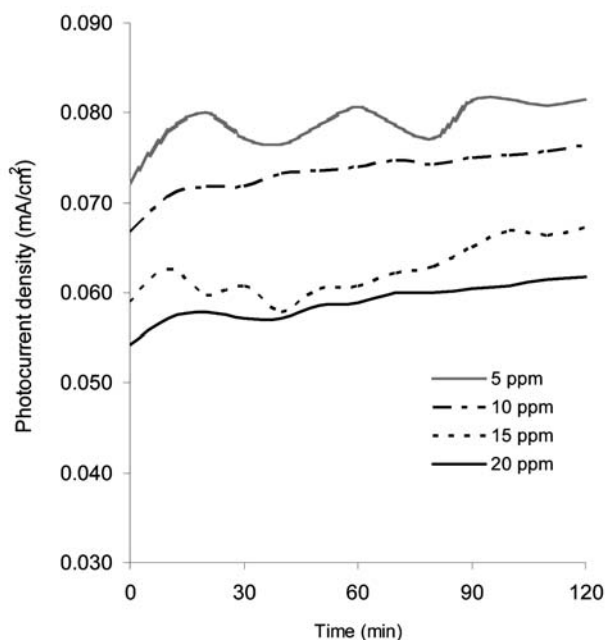


**Figure 11.** Charge density and specific removal for methyl orange at different coated electrode area.

Figure 11 shows that the specific removal of methyl orange by photoelectrochemical degradation is the highest for coated electrode area of 7 cm<sup>2</sup>. This indicates although charge density is low for large coated area electrode but it is rather efficient in degrading the dye. Therefore, coated area of 7 cm<sup>2</sup> shows high efficiency in consumption of photon generated from light sources in degrading the dye. It is possible to infer that the photocurrents, which were generated from oxidation process such as photooxidation of water and other species in the solution did produce oxidising species on adsorbed surface or into bulk solution, but not all species are favourable for photodegradation. Thus, the photocurrent is not always proportional to the electrode capability in degrading the dye. In addition, the

surface bound oxidising species seems to play more important role in degrading the dye because the specific removal was enhanced when the photocatalyst coated area was increased.

## 4. Conclusions

This study has demonstrated that heat treatment greatly influence the properties of the electrode. Crystallinity, surface characteristic, adhesion and photocatalytic activity of TiO<sub>2</sub> were improved by applying the heat treatment. The study shows that methyl orange was degraded efficiently after an irradiation time of 120 min using electrode heat-treated at 500 °C. Applying bias potential successfully promotes photoelectrocatalytic degradation rate. The selected potential (in this study was ≤1.5 V) was significantly important to avoid the existing dark current which leads to direct dye degradation. Investigation on the effect of dye concentration shows that the percentage of degradation decreased with increasing dye concentration. This indicates the consistency of the electrode in the aspect of degradation certain amount of dye. Increasing areas of coated TiO<sub>2</sub> increase the surface for reaction event-hough this reduces charge density. This is shown by the highest electrode coated area of 7 cm<sup>2</sup> successfully degraded 5.27 × 10<sup>-7</sup> mol of dye (per unit area) with charge density of 5.34 C cm<sup>-2</sup>.

## 5. Acknowledgments

We gratefully acknowledge the financial support from the Malaysian Government through the IRPA programme no: 09-02-04-0255-EA001 and 09-02-04-0369-EA001.

## 6. References

1. D. A. Tryl, A. Fujishima, K. Honda, *Electrochim. Acta* **2000**, *45*, 2363–2376.
2. A. Fujishima, T. N. Rao, D. A. Tryk, *J. Photochem. Photobiol. C: Photochem. Rev.* **2000**, *1*, 1–21.
3. J. A. Bryne, A. Davidson, P. S. M. Dunlop, B. R. Eggins, *J. Photochem. Photobiol. A: Chem.* **2002**, *148*, 365–374.
4. C. Feng, N. Sugiura, S. Shimada, T. Maekawa, *J. Harzard. Mater.* **2003**, *103*, 65–78.
5. F. Haque, E. Vaisman, C. H. Langford, A. Kantzas, *J. Photochem. Photobiol. A: Chem.* **2005**, *169*, 21–27.
6. R. L. Pozzo, M. A. Baltanas, A. E. Cassano, *Catal. Today* **1997**, *39*, 219–231.
7. M. A. Barakat, Y. T. Chen, C. P. Huang, *Appl. Catal. B: Env.* **2004**, *53*, 13–20.
8. M. R. Hoffman, S. T. Martin, W. Y. Choi, D. W. Bahnemann, *Chem. Rev.* **1995**, *95*, 69–96.

9. A. Piscopo, D. Robert, J.V. Weber, *J. Photochem. Photobiol. A: Chem.* **2001**, *139*, 253–256.
10. J. A. Bryne, B. R. Eggins, N. M. D. Brown, B. McKinney, M. Rouse, *Appl. Catal. B: Environ.* **1998**, *17*, 25–36.
11. A. Blozkow, I. Csolleova, V. Brezova, *J. Photochem. Photobiol. A: Chem.* **1998**, *113*, 251–256.
12. K. Vinodgopal, S. Hotchandani, P. V. Kamat, *J. Phys. Chem.* **1993**, *97*, 9040–9044.
13. K. Vinodgopal, U. Stafford, K. A. Gray, P. V. Kamat, *J. Phys. Chem.* **1994**, *98*, 6797–6803.
14. J. Luo, M. Hepel, *Electrochem. Acta* **2001**, *46*, 2913–2922.
15. X. Z. Li, F. B. Li, C. M. Fan, Y. P. Sun, *Wat. Research* **2002**, *36*, 2215–2224.
16. S. Zhang, H. Zhao, D. Jiang, R. John, *Anal. Chimica Acta* **2004**, *514*, 89–97.
17. K. Vinodgopal, P. V. Kamat, *Sol. Energy Mater. Sol. Cells* **1995**, *38*, 401–410.
18. K. Kato, A. Tsuzuki, Y. Torii, H. Taoda, *J. Mater. Sci.* **1995**, *30*, 837–841.
19. K. Kato, A. Tsuge, K. Niihara, *J. Am. Ceram. Soc.* **1996**, *79*, 1483–1488.
20. K. Kato, K. Niihara, *Thin Solid Films* **1997**, *298*, 76–82.
21. D. R. Ulrich, *Chemtech*, **1998**, *April*, 242.
22. M. T. Colomer, J. R. Jurado, *Chem. Mater.* **2000**, *12*, 923–930.
23. X.-Z. Ding and X.-H. Liu, *J. Mater. Res.* **1998**, *13*, 2556–2559.
24. B. D. Cullity, *Elements of X-Ray Diffraction*, 2nd ed., Addison-Wesley, Reading, MA, **1978**, pp. 102.
25. D. L. Jiang, H. J. Zhao, Z. B. Jia, J. Cao, R. John., *J. Photochem. Photobiol. A: Chem.* **2001**, *144*, 197–204.
26. T. Yoko, A. Yuasa, K. Kamiya, S. Sakka, *J. Electrochem. Soc.* **1991**, *138*, 2279–2284.
27. T. Yoko, L. Hu, H. Kozuka, S. Sakka, *Thin Solid Films* **1996**, *283*, 188–195.
28. K. Mizushima, M. Tanaka, A. Asai, S. Iida, J. B. Goodenough, *J. Phys. Chem. Solids* **1979**, *40*, 1129.
29. R. Pelegrini, P. Peralta-Zamora, A. R. Andrade, J. Reyes, N. Duran, *Appl. Catal. B: Env.* **1999**, *22*, 83–90.
30. C. C. Sun, T. C. Chou, *J. Mol. Catal. A* **2000**, *151*, 133–145.
31. Z. Zainal, C. Y. Lee, M. Z. Hussein, A. Kassim, N. A. Yusof, *J. Photochem. Photobiol. A* **2005**, *172*, 316–321.
32. M. Hepel, J. Luo, *Electrochem. Acta* **2001**, *47*, 729–740.
33. P. S. M. Dunlop, J. A. Bryne, N. Manga, B. R. Eggins, *J. Photochem. Photobiol. A: Chem.* **2002**, *148*, 355–363.
34. B. Neppolian, H. C. Choi, S. Sakthivel, B. Arabindoo, V. Murugesan, *J. Hazard. Mater. B* **2002**, *89*, 303–317.
35. C. Galindo, P. Jacques, A. Kalt, *J. Photochem. Photobiol. A: Chem.* **2001**, *141*, 47–56.

## Povzetek

Z metodo sol-gel priprave premazov smo pripravili tankoplastne filme  $\text{TiO}_2$ . Kemijsko spremenjene sol-gel raztopine prekurzorjev smo dobili z dodatkom polietilenglikola in dietanolamina, ki v prisotnosti vode reagirata s titanovim alkoksidom s pomočjo kontrolirane hidrolize in polikondenzacije. Elektrokemično spodbujeno fotokatalitično razgradnjo sistema smo raziskovali z modelnim onesnaževalom, barvilom metil oranž. Lastnosti filma smo določili kot funkcijo temperature kalcinacije z raziskavami površinske morfologije, difrakcijo X-žarkov in fotoelektričnimi raziskavami. Hitrost fotokatalitičnih procesov znatno naraste pri uporabi zunanjšega bias potenciala. Kot lahko razberemo iz odvisnosti toka od napetosti, se neposredna oksidacija barvila začne pri potencialu 1.5 V zaradi temnega toka. Uporaba višje koncentracije barvila vodi do zmanjšanja deleža fotorazgradnje, vendar hitrost fotoelektrokemične razgradnje ostaja skoraj enaka. Pri večji površini fotokatalizatorja opazimo večjo hitrost razgradnje, vendar manjšo gostoto naboja.